J Mater Sci (2007) 42:7275–7285
DOI 10.1007/s10853-006-1484-7

The role of gas penetration on morphological formation of polycarbonate/polyethylene blend molded by gas-assisted injection molding

Guo-Qiang Zheng · Wei Yang · Li Huang · Zhong-Ming Li · Ming-Bo Yang · Bo Yin · Qian Li · Chun-Tai Liu · Chang-Yu Shen

Received: 27 July 2006 / Accepted: 22 December 2006 / Published online: 10 May 2007

Abstract Polycarbonate (PC)/polyethylene (PE) blend was molded respectively by short shot (SS) and gas-assisted injection molding (GAIM). In order to investigate the origin of the ''skin-core'' structure during GAIM process, the morphology of the two parts molded by SS and GAIM, far from skin, was studied. The results indicate that the structure of the SS part (SSP) is similar to that molded by conventional injection molding (CIM), while the structure of the GAIM part (GAIMP) shows an unusual gradient structure. Many coarse, short PC fibrils arise in sub skin, while such fibrils become more well-defined and reduce in number towards core layer. And the PC phase at the non-gate end, experiences more severe deformation than that at the gate end, which is also different from that in CIM parts. In addition, Moldflow 5.1, a commercial simulation package, was employed to determine the flow behaviors during SS and gas penetration processes. The experimental and simulated results indicate that shear rate and cooling rate are significant for the gradient structure formation during GAIM.

G.-Q. Zheng · W. Yang · L. Huang · Z.-M. Li · M.-B. Yang (✉) · B. Yin
College of Polymer Science and Engineering, State Key Laboratory of Polymer Materials Engineering, Sichuan University, Chengdu 610065, P.R. China
e-mail: yangmb@scu.edu.cn

Q. Li · C.-T. Liu · C.-Y. Shen
National Engineering Research Center for Advanced Polymer Processing Technology, Zhengzhou University, Zhengzhou 450002, P.R. China

Introduction

Gas-assisted injection molding (GAIM) [1, 2], an innovative injection molding process illustrated in Fig. 1, has attracted intensive attention in the past years. This process came into practice widely as a ripe technology in 1990s, and has been spread extensively, mounting up to 10% of CIM [3]. During GAIM process, the mold cavity is partially filled with melt followed by the injection of compressed gas. Compressed gas penetrates into the melt and forces it to fill the whole mold cavity [4–7]. GAIM has many advantages. For example, it can reduce operating expenses by saving material cost, reducing clamp tonnage and cycle time. Above all, the mechanical properties and macro-qualities can be greatly improved because of reduction in residual stress, warpage, sink marks, shrinkage and so on.

Despite these advantages associated with GAIM, the molding design and process control become more critical and difficult since this process involves dynamic interaction between two dramatically dissimilar materials flowing within the mold cavity. Therefore, previous experiences with CIM become insufficient to deal with GAIM, especially when describing the morphological development in the parts molded by GAIM.

In view of its intrinsic advantages, a great deal of work has been carried out on GAIM. So far, fundamental studies mainly concerned the mathematic simulation of gas penetration [8–14], the effect of the gas channel design on the gas penetration behavior [4, 7, 14, 15], molding windows [4, 16, 17], the influence of gas channel shape on the mechanical properties [18–20] and so on. For the microstructure of GAIM parts, Chien [18] explored the crystallinity of polyamide (PA) while studying the effect of gas channel shape on the mechanical properties of GAIM

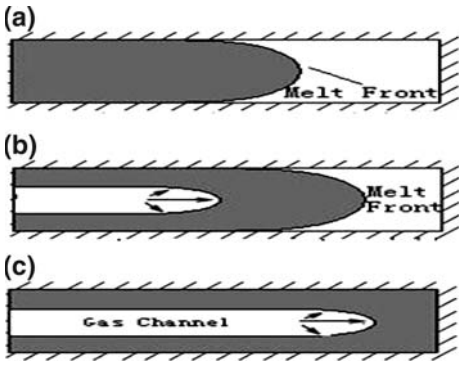

Fig. 1 Schematic diagrams of GAIM process. (**a**) partial melt filling; (**b**) gas penetration; (**c**) gas-assisted packing

moldings. Because of the higher degree of crystallinity, the maximum tensile load and the ultimate tensile stress of PA moldings exhibited significant dependence on part thickness. However, studies on the morphology in GAIM parts are very limited. Though our previous study [21] revealed the morphology difference in the GAIM part and CIM part, but the origin of morphology development during gas penetration was still unclear.

Therefore, the morphology in the part molded by GAIM and in that molded by SS was explored. The results might be helpful to fully understand the mechanism of the ''skin-core'' structure formation during GAIM.

Experimental

Materials

The resins used in this study were PC and HDPE. PC (Model K1300) with a number-average molecular weight of 2.8–3.2 $\times 10^4$ g mol^{-1} and a molecular weight distribution index of 2.1, derived from bisphenol A, was obtained from Teijin Chemical Co.Ltd., Japan. The HDPE (Model 5000S) was a commercial product of DaQing Petroleum Chemical Co., China, supplied in pellets with a melt flow rate (21.6N, 190 °C) and number-average molecular weight of 0.9 g·(10 min)$^{-1}$ and 5.28 $\times 10^5$ g ·mol^{-1}, respectively.

Preparation of samples

PC was dried under vacuum at 100 °C for at least 12 h before dry-mixing with PE with a fixed weight ratio of 20/80, in order to avoid its hydrolytic degradation in the following processing. The mixture was then blended in a TSSJ-25 twin-screw extruder with a temperature profile of 150, 190, 230, 265, 275, and 270 °C from hopper to die. The rotation speed of the screw was maintained at 120 rpm. The extrudate was palletized and dried before molding.

A Grand 140–320 injection molding machine and a gas injection system (model MPC) with five-stage pressure profile control were employed for the molding process. In this work, only one stage of gas injection was used. The processing parameters of gas-assisted molding are listed in Table 1. Two kinds of parts were molded respectively by GAIM and SS process. The part molded by GAIM was referred to as GAIMP and the part molded by SS was nominated as SSP. In this study, GAIMP and SSP were of same processing condition, except that SSP was not exposed to the gas penetration and gas-assisted packing process. The injection volume was about 85% for SSP, the same to GAIMP. The geometry of the mold cavity is shown in Fig. 2. The gate of the mold used had been also optimized compared to that used in our previous study [21], thus some disadvantages such as ''jetting'' can be avoided. Since SS is a necessary process for GAIM, the morphology formed respectively in these two processes might be somewhat related, which is the main reason that two kinks of parts were fabricated respectively by SS and GAIM.

Morphological observation

In order to get the surfaces for scanning electron microscope (SEM) observation, the parts were cut into a short segment (about 3 mm in length) from the shadows (see Fig. 3), namely at the gate end and non-gate end, on SSP and GAIMP. These specimens and the PC/PE blend thread extruded were put into liquid nitrogen for about 40 min,

Table 1 The GAIM parameters used

Parameters	Values
Injection pressure (MPa)	80
Gas Packing pressure (MPa)	11.032
Delay time (s)	1
Gas packing time (s)	10
Cool time (s)	60
Melt temperature (°C)	280
Mold temperature (°C)	30

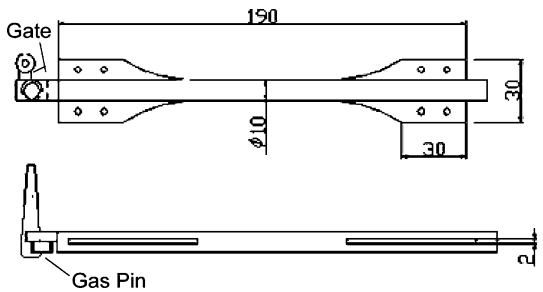

Fig. 2 Geometry of the mold cavity used

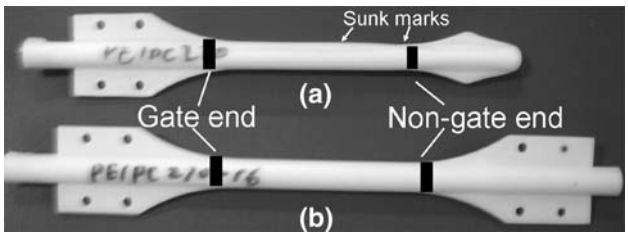

Fig. 3 Macro-photos of the SSP and GAIMP. (**a**) SSP; (**b**) GAIMP

and then quickly broken along the flow direction by impact to make surfaces for SEM observation. Before observation, the specimens were gilded in a vacuum chamber to make them conductive. The morphology was observed on an SEM instrument, JSM-5900LV, operating at 20 kV.

Results and discussion

Macro-photographs of SSP and GAIMP

The macro-photographs of GAIMP and SSP are shown in Fig. 3. It is found that SSP had shrunk intensively as many sunken marks of strip form appeared on its surface. The lack of melt during SS process (see Fig. 1a) and the absence of packing pressure at the end of SS process account for this case. After the end of SS process, the melt injected into the cavity stopped flowing because there is no extra melt continues to enter the cavity. A thin layer of SSP was cooled down by the mold wall, while most interior polymer of the SSP was still in the melt state because the interior melt was deficient in heat exchange with the cool mold wall. Since there is no packing pressure like that in CIM, hereby there was no enough melt to compensate for the shrinkage during cooling. Consequently, sunken marks appeared on the surface of SSP. As for GAIMP, a perfect appearance was obtained and shrinkage was almost avoided as the compressed gas continued to pressurize the melt to cling to mold wall till the melt was frozen absolutely during GAIM process.

Original morphology of PC/PE blend

Figure 4 shows the SEM micrograph of the PC/PE blend extruded from the die. It is obvious that the dispersed phase mainly assumed spherical form, with the size exhibiting a range of distribution, which could be as large as 1.5 μm, and as small as 0.2 μm. Some of the PC particles were embedded in the PE matrix and the others were pulled out during sampling, leaving many grooves in the matrix. The interfaces between PC and PE were very smooth and there was scarcely evidence of adhesion, implying that the two resins were severely incompatible.

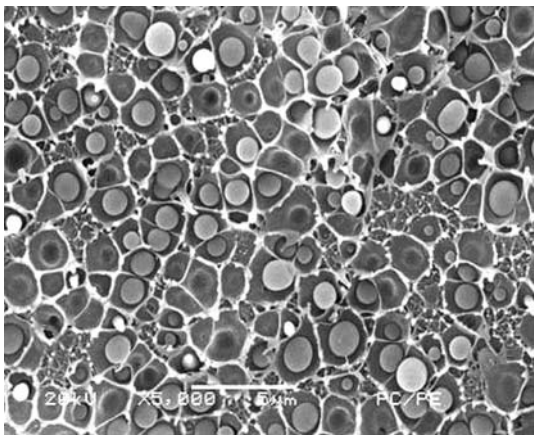

Fig. 4 Original morphology of the PC/PE blend after extruded

Morphology of SSP

SEM micrographs of the SSP over the section, from skin to core layer at the gate end and non-gate end, in the melt flow direction are presented in Fig. 5. The regions where Fig. 5a–c, 5a′–c′ were obtained are presented in Fig. 6. For convenience, we designate the mold wall/polymer interface as skin. The skin is neglected because there is no dispersed phase in it.

According to the degree of deformation, the morphology of SSP includes three layers, sub skin, sub-skin intermediate layer as well as core layer, perpendicular to the melt flow direction. It is noticeable that there are some slim PC fibrils, grooves left by fallen fibrils and a few PC bars in sub skin (see Fig. 5a) at the gate end. In sub skin at the non-gate end, more coarse and fine fibrils came into being (see Fig. 5a′). Not only at the gate end but also at the non-gate end, all the micro-fibers in sub skins inclined to orientate along the flow direction. As shown in Fig. 5b, 5b′, PC phase primarily assume the rod-like shape in sub-skin intermediate layers at both ends, and the two regions are also dotted with many spheres and humped ellipses. But there are more bars of various shapes in Fig. 5b than those in Fig. 5b′. It is obvious that the bars in Fig. 5b′ are more dumpy than those in Fig. 5b. At both ends, PC spheres of different sizes dominate the core layer. The bars pointed by the white arrows in Fig. 5b and Fig. 5b′, seem to be linked by several independent particles during filling. Though the melt velocity field in the cavity is very complex in the melt filling, the velocity from the gate end to the non-gate end must be continuous since a single-side gate was used in this study.

According to the morphology at both ends of SSP, the following results could be obtained:

(1) In the same layer, PC phase at the gate end was, generally, deformed to a larger degree than that at the

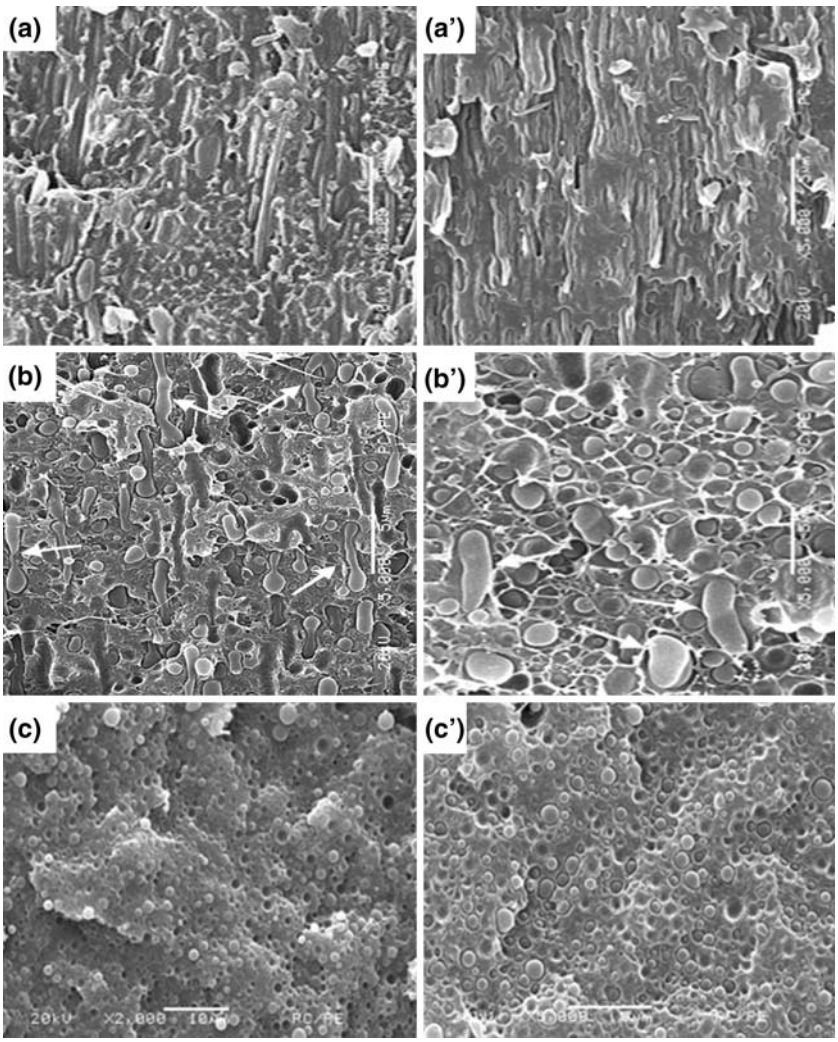

Fig. 5 SEM micrographs at different positions of SSP. (**a**) and (**a′**) sub skin; (**b**) and (**b′**) sub-skin intermediate layer; (**c**) and (**c′**) core layer

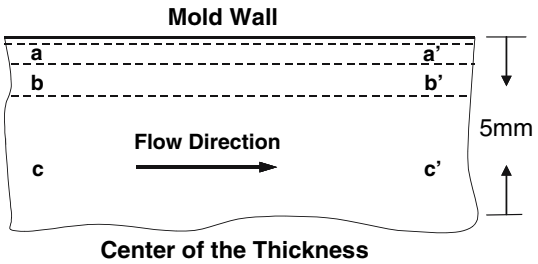

Fig. 6 Schematic representation of the regions where Fig. 5**a**–**c**, and 5**a′**–**c′** were obtained on the cryogenically fractured surface (**a**, **b** and **c**: gate end; **a′**, **b′** and **c′**: non-gate end)

non-gate end, which indicated that PC particles experienced much fiercer shear or elongation stress at the gate end.

(2) PC bars at the gate end ranked more orderly than that at the non-gate end. Besides, more PC bars were formed at the gate end than that at the non-gate end.

Morphology of GAIMP

SEM micrographs of GAIMP in the regions in flow direction, from sub skin to gas channel layer at both ends are presented in Fig. 7. The regions where the pictures labeled a–d, and a′–d′ were obtained are shown in Fig. 8. Skin is also neglected here.

According to the degree of deformation, morphology of GAIMP includes five layers perpendicular to the melt flow direction. They are sub skin, sub-skin intermediate layer, core layer, core intermediate layer and gas channel layer.

As shown in Fig. 7a, in sub skin, a few bars of different forms, spheres and fibrils coexisted at the gate end, while more slim and coarse fibrils are dominant (see Fig. 7a′) at the non-gate end. Many bulky fibrils, with smooth bumps on their surfaces appeared in sub-skin intermediate layer, as presented in Fig. 7b. Though the Fig. 7b′ is not clear for the poor gilding before SEM observation, the fibrils, which were similar to those in Fig. 7b are still observed vaguely.

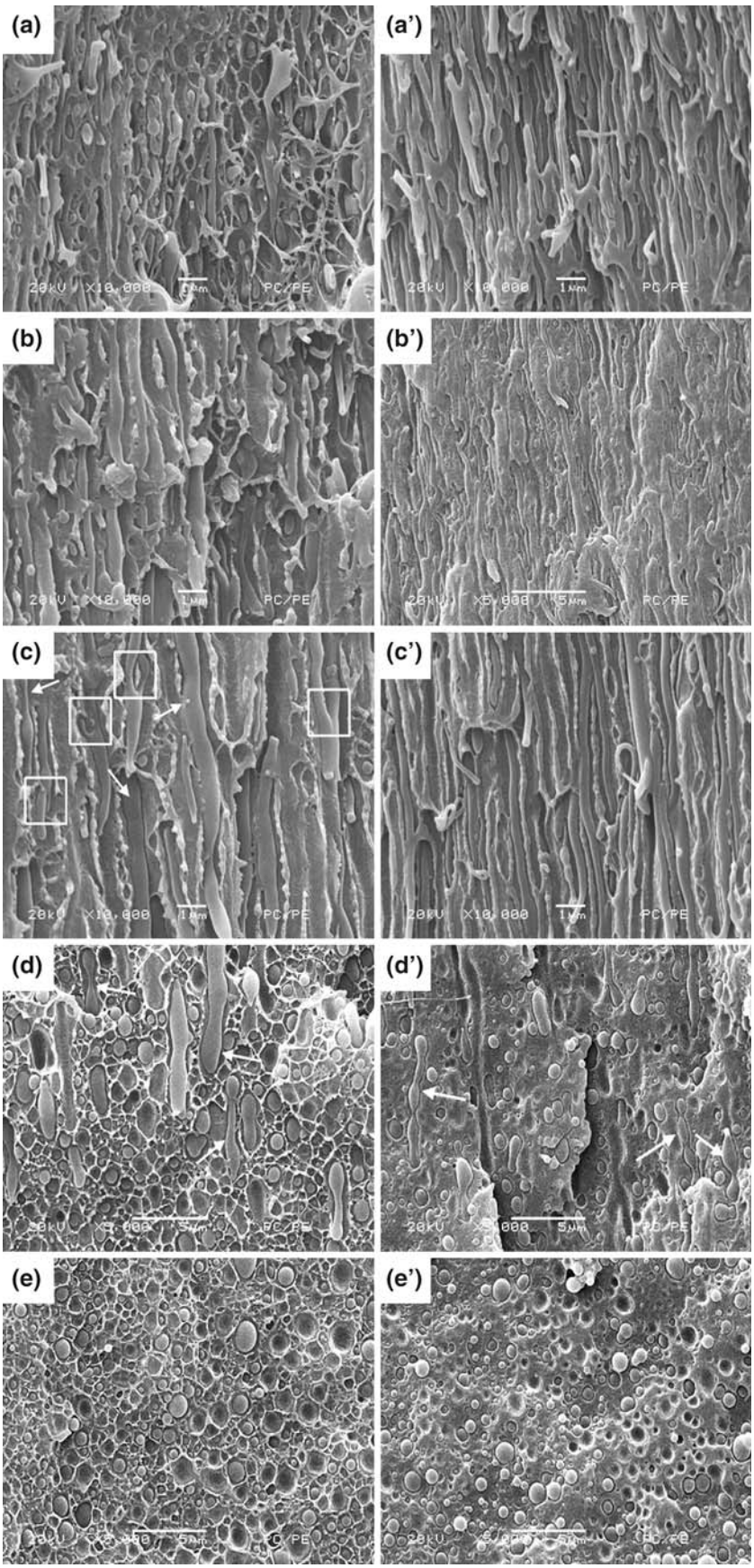

Fig. 7 SEM micrographs at different regions of GAIMP. (**a**) and (**a′**) sub-skin; (**b**) and (**b′**) sub-skin intermediate layer; (**c**) and (**c′**) core layer; (**d**) and (**d′**)gas-channel intermediate layer; (**e**) and (**e′**)gas-channel layer

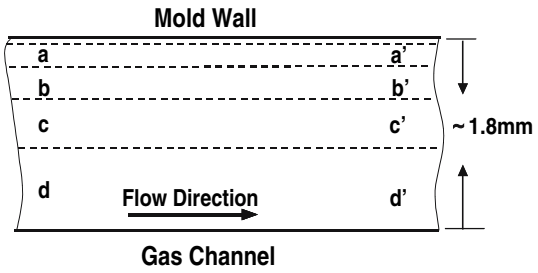

Fig. 8 Schematic showing of the regions where Fig. 7**a**–**d**, and 7**a′**–**d′** were obtained on the cryogenically fractured surface (**a**, **b**, **c**, **d** and **e**: gate end; **a′**, **b′**, **c′**, **d′** and **e′**: non-gate end

At both ends, it is apparent that numerous well-defined micro-fibers were embedded in the core layer (see Fig. 7c, 7c′), while the PC phase in Fig. 7c′ exhibited a severer deformation than that in Fig. 7c. And the fibrils were too long to be fully observed in the range of both pictures. Interestingly, a few branches were derived from the body of the micro-fibers shown by the white rectangles in Fig. 7c. It might imply that the fibrils are probable to impinge with other PC spheres or fibrils during gas penetration process, which could partially explain why the fibrils, in the core layers, are longer and more continuous than those in sub skin. Another reason may be the non-uniform distribution of PC particles from sub skin to core layer during filling. The PC particles in sub skin were smaller in size and scarcely had chance to touch with others during deformation, and just turned into shorter fibrils when exposed to shear field. Notwithstanding, it also seems that many fibrils were broken and pull out during sampling, and that a few fractured surfaces of the fibrils and a few grooves left. On the whole, the diameter of fibrils in Fig. 7c is a little larger than that in Fig. 7c′, while the microfibers in Fig. 7c′ were much denser than those in Fig. 7c. In gas-channel intermediate layers, there appeared more PC spheres and bars with irregular forms at both ends (see Fig. 7d, 7d′). Interestingly, several ''strings of beads'', pointed by the white arrows, arose unexpectedly in the above two layers, especially at the non-gate end. However, well-defined spheres were dominant in gas channel layer (Fig. 7e, 7e′).

In a word, the morphology inside GAIMP was apparently heterogeneous and anisotropic, generally assuming a typical skin-core distribution. The following conclusions could be drawn by comparing the morphology of each layer at both ends:

(1) Not only at the gate end but also at the non-gate end, PC phase is of lager deformation in the core layer than that in the other layers
(2) Except in gas channel layer and sub-skin layer, PC phase at the non-gate end has a far more drastic shape change than that at the gate end in each layer. Especially in the core layer, PC fibrils at the non-gate end have smaller diameter and aligned more orderly than those at the gate end. On the whole, the morphology at the non-gate end was of greater degree deformation than that at the gate end.

Morphology comparison between the SSP and GAIMP

During SS process, the melt are surrounded by cool mold wall and unfilled cavity. In such process, the orientated phases always tend to relax and shrink because of shortage of melt and higher temperature in the center of the mold cavity. As shown in Fig. 1, GAIM involves SS process. However, they are remarkably different because the melt during gas penetration is confined not only by the mold wall and the unfilled cavity, but also by the compressed gas (see Fig. 1b). The gas is efficient in transmitting the pressure required to move the viscoelastic melt, which is quite different from that in SS and CIM process. Such difference may lead to different flow and rheological behaviors. The two different processes mentioned may bring about the following morphological difference between SSP and GAIMP.

(1) In SSP, PC phase underwent the greatest deformation in sub skin, while PC phase of GAIMP deformed severest in sub-skin intermediate layer and core layer;
(2) For the same layer (such as sub skin, sub-skin intermediate layer) in SSP, the diameter of dispersed phase at the gate end is generally smaller than that at the non-gate end. Whereas, the diameter of PC phase at the gate end, in the same layer (such as sub skin intermediate layer and core layer) of GAIMP, is slightly larger than that at the non-gate end;
(3) Generally, the effect of fibrillation in GAIMP is much more profound than that in SSP.
(4) The morphology in sub skins of GAIMP and SSP has no obvious difference.

The mechanisms of the morphological formation in GAIMP

It is well known that the skin-core structure of the blends molded by CIM is chiefly ascribed to the orientation of dispersed phase along the complex melt flow lines during melt filling. Simultaneously, the ''fountain flow'' pattern also occurs at the melt front [22, 23]. In this case, the melt front is cooled by contact with ''cool'' air, and therefore, becomes highly viscous. Driven by the melt at the centre of the flow channel, the melt is rearranged on the flow front from inwards to outwards. Hence, the PC phase in the melt

front is stretched in elongational field induced by fountain flow [24, 25]. Once the deformed PC phase contacts the cool wall of the mold, it will be frozen immediately and then reserved. As shown in Fig. 1a, SS process is quite similar to the filling phase of CIM. The distinct difference between them is that the former has no enough melt to fill the whole cavity. Accordingly, the mechanism of morphological formation in SSP and the parts molded by CIM are very alike. Consequently, the elongational flow on the fountain flow front results in the fibrils formation in sub skin of SSP. Because the origin of the morphological development for PC/PE blend in the CIM part had been explored profoundly by Li [26], therefore, there is no need for us to repeat it.

In order to fully understand the morphological formation of GAIMP, the flow behaviors were simulated under the same conditions as those in practical process, employing the commercial CAE software packages, namely Mold flow 5.1.

According to the simulated results, it takes about 9.82 s for melt to fill the cavity during SS process. Additionally, the velocity and shear rate in the cross sections of the both ends (showed by black rectangles in Fig. 3a) were obtained from the simulated results (t = 9.5 s) just before melt fulfilled the filling process. Due to symmetry, the results for half the thickness of specimen are shown. It can be seen from Fig. 9 that velocity at both ends has no remarkable increase in the region about 1 mm away from the skin. Then, it begins to increase rapidly till the center zone. The velocity is as large as 5.4 cm/s at the gate end and 4 cm/s at the non-gate end. At both ends, shear rate (see Fig. 10) shows a steep increase from the skin to the region about 0.7 mm away. Then, it begins to decrease slowly till the center zone. Shear rate is as large as 22.8 s^{-1}at the gate end and 14 s^{-1} at the non-gate end.

According to the simulated result, it cost about 0.05 s (from 10.83 s to 10.88 s) to finish the primary gas

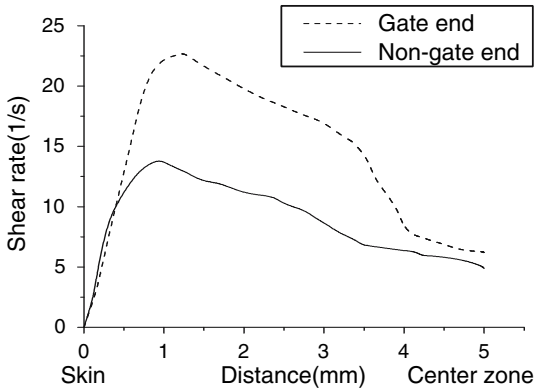

Fig. 10 The shear rate in the cross section at both ends during SS process (t = 9.5 s)

penetration. When gas front is about to reach the gate end (left black rectangle in Fig. 3b, t = 10.84 s) and the non-gate end (right black rectangle in Fig. 3b, t = 10.87 s), the velocity and shear rate in the cross sections of both ends are obtained at these moments, respectively. As presented in Fig. 11, velocity primarily keeps 0 cm/s till 0.6 mm away from the skin. Then it increases abruptly from 0 cm/s to 2280 cm/s at the non-gate end, and 1067 cm/s at the gate end. The shear rate in the cross section at both ends during gas penetration process (t = 10.84 s and 10.87 s) is illustrated in Fig. 12. At the gate end, shear rate rises precipitously from 0 s^{-1} to 4832 s^{-1}. It reaches the maximum about 2 mm away from the skin. Then, it starts to decline from 4832 s^{-1} to 2441 s^{-1} in the center zone. However, the shear rate at the non-gate end show an abrupt increase from the skin to about 0.4 mm further, and then decrease to its minimum (2920 s^{-1}) in the center zone.

Based on the above description, it can be found that many differences in flow behaviors during SS process and gas penetration process: ① At the points with the same distance from the skin, both velocity and shear rate at the

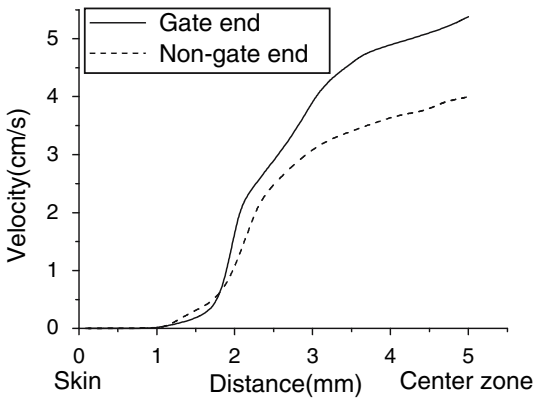

Fig. 9 The velocity in the cross section at both ends during SS process (t = 9.5 s)

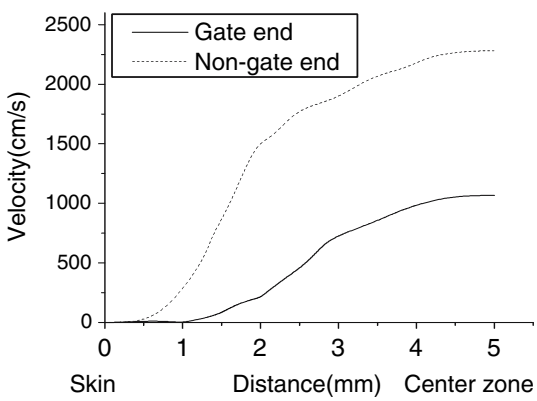

Fig. 11 The velocity in the cross section at both ends during gas penetration process (t = 10.84 s and 10.87 s)

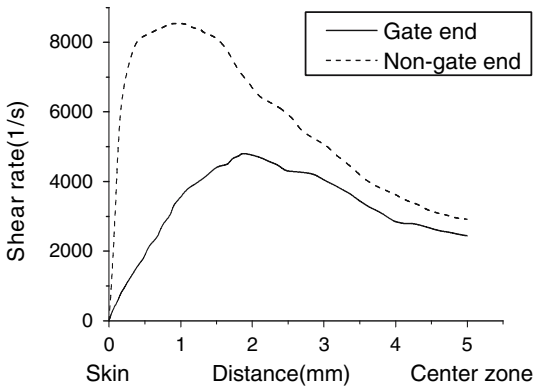

Fig. 12 The shear rate in the cross section at both ends during gas penetration process (t = 10.84 s and 10.87 s)

gate end were generally larger than those at the non-gate during SS process, while reversal results could be obtained during gas penetration process. ② During gas penetration process, velocity and shear rate at both ends are obviously larger than those in the corresponding regions in SS process. Furthermore, it could be noted that the flow behaviors during SS process are similar to that [26–29] in CIM process. Here, we prefer to make clear the unusual flow behaviors in GAIM process rather than paying more attention to the morphological formation in SS process. The reasons why there are so many differences between the two processes might be as follows. Before penetration, the gas used must flow from a gas injection system, through a steel pipe, to the gas pin fixed in the mold cavity. Thus, gas pressure might not be the predetermined one when the gas enters the melt at the gate end. However, the gas pressure would increase sharply and reach the settled one during penetration. In consequence, owing to the different gas pressure at both ends, velocity and shear rate at the non-gate end are different from those at the gate end. The shear rate and velocity at the non-gate end would be strengthened by the higher gas pressure as well. In addition, the melt ahead the gas front must advance faster than that during SS process since gas is efficient in transmitting pressure. Therefore, velocity and shear rate during the GAIM process was higher than those in the SS process. Hence, it is easy to understand the different morphological formation at both ends of GAIMP. Though the results from the simulation could not precisely reflect the practical processing process, they might provide a general picture of flow behaviors in the processing processes and enhance our understanding of the gradient structure in GAIMP.

In this investigation, the melt filled the cavity from the gate end to the non-gate end successively because a side-single-gate mold was designed and the ''jetting'' is avoided. As mentioned above, distinct differences in flow behaviors between GAIM and SS process may determine the different morphology of GAIMP and SSP. In GAIM, melt first advances in SS process (see Fig. 1a), and then impelled by gas, it starts to flow once more at the end of delay time (see Fig. 1b). The gradient structure of GAIMP hereby is mainly fabricated in these two processes. According to the above simulated results, it is easy for us to understand the gradient structure. Additionally, the compressed gas is the only power to propel the melt forwards after the SS process. In view of this, we conjecture that the gradient morphology formation from sub skin intermediate layer to gas channel layer of GAIMP might be ascribed to gas penetration.

The morphology evolution to the final solid-state structure after injection molding is determined by the flow fields experienced by the melt during mold filling, and the cooling rate during and after mold filling. In sub skin and sub skin intermediate layer of SSP, shear rate is relatively high and thus micro-fibers could be formed. Besides, the cooling rate in these regions is rapid enough to freeze the fibrils before any relaxation could occur. Shear rate in core layer of SSP is minimal and hence fibrils could not form easily. Furthermore, in SSP, it is about 5 mm away from core layer to skin, so heat in core layer could not dissipate efficiently. Therefore, relaxation might occur because heat can not dissipate efficiently and thus PC phase primarily exhibits spherical form.

As discussed above, sub skins in SSP and GAIMP near the mold wall, and the cooling rate is rapid enough to preserve the morphology formed before any relaxations occur. Since the melt in sub skin is cooled down once it contacts the mold wall during SS process, and then the morphology in this region of GAIMP is scarcely influenced by gas penetration. In other words, the morphology formation in sub skins of GAIMP and SSP is of the same mechanism. The similarity of morphology in sub skins of GAMIP and SSP is a forceful evidence to substantiate our judgment.

In sub skin intermediate layers (about 0.4 mm away from skin) at both ends of GAIMP, shear rate is relative higher (Fig. 12), and hence, morphology in terms of long continuous fibrils is formed in the regions as expected. The fibrils at the non-gate end show more serious deformation than those at the gate end, because of the higher shear rate at the non-gate end (Fig. 12).

The shear rate in the core layers (about 0.8 mm away from skin) at both ends of GAIMP is also relative higher, which results in obvious morphological deformation in these regions. Because of the higher shear rate experienced at the non-gate end (Fig. 12), the fibrils at the non-gate end show more intensive deformation than those at the gate end.

Though in gas channel intermediate layers and gas channels layers, the shear rate is somewhat lower than that

in the core layers, yet, it is quite high according to the simulated results. The dispersed phase in these regions, therefore, should be deformed more seriously as expected. However, fewer fibrils are formed in these regions. So it seems paradoxical that higher shear rate and rapid cooling rate could not give rise to fibrillar formation in these regions. It is well known that the final morphology of the injection-molded bar is the product of the balance between deformation, breakup and coalescence. Since gas channel layer is about 1.8 mm away from the cool mold wall, if PC fibrils could be formed in these layers, the cooling rate is still rapid enough to preserve the fibrils that had been formed. Additionally, excessive shear rate may cause the breakup of fibrils and turn them into shorter fibrils or particles. Even thought both shear rate and cooling rate in core layer are larger than those in gas channel intermediate layer and gas channels layer, no evidence of breakup is found in core layer (see Fig. 7c′). According to the above discussion, a conclusion can be drawn: practical shear rate in core layer, gas channel intermediate layer and gas channels layer is not as large as the simulated results. Shear rate in gas channel intermediate layer and gas channels layer is too small to deform PC phase. And shear rate in core layer only can transform PC phase into fibrils, but it is not enough to break them up.

Liu [30] investigated the fiber orientation in the water-assisted injection molded PP which was filled with glass fiber, and found that fibers highly oriented in the regions near the mold wall and the water channel rather than in the center of the thickness. Why does not the fibrillation of PC/PE blend occur in the gas channel layer, which is close to the gas channel? The mediums (water and gas) used, with entirely different physical properties, used respectively in water-assisted injection molding and GAIM might give us some promising clues to explain such phenomenon. Generally, the gas used is regarded as ''inert gas'', and there is no reaction with polymer. As a result, the compressed gas merely propels the melt around the gas front forward during the gas penetration process, and will not draw the melt adjacent to the gas channel forward. On the other hand, gas has an intrinsic smaller frictional coefficient, especially under the supercritical condition [31], and hereby there is hardly friction between the gas channel layer and the gas. Thus, gas flow can not draw the melt adjacent to the gas channel forward, and the dispersed phase in the gas channel layer will not be elongated and fiberized by the gas flow. Thus we assume that shear rate in these region are not as high as the simulated results present, by which fibrillar form could not be induced. However, that is just some speculation on such phenomenon, with further study in this area waiting to be carried out.

It is noted that the rheological and interfacial properties, the viscosity ratio, the blend composition, the mixing parameters and the mixing mode are the governing factors to determine the morphology of dispersed phase during blending and processing. Moreover, an elongational flow and a low viscosity ratio (less than or close to unity) of the dispersed phase and matrix are beneficial to the fibrillation of the dispersed phase particles in an immiscible polymer blend [32–34]. Generally, the viscosity of PC is much higher than that of matrix HDPE, resulting in a viscosity ratio much higher than unity, which does not facilitate the fibrillation of PC phase in HDPE matrix [35]. Except for sub skin of GAIMP, shear flow is dominant in other layers. According to the above discussion, the PC phase should be deformed slightly. Unexpectedly, denser and more intensive deformed fibrils are formed in GAIMP. Such phenomenon arouses our curiosity to further probe the fibrillation of PC/PE blend induced by gas penetration during GAIM. Suppose that a single fibril of the SSP and GAIMP was derived from an independent PC particle, and then the fibril and the PC particle must be of the same volume during the deformation. If the PC particles in the extrudate (Fig. 4) and fibrils in the SSP and GAIMP are respectively regarded as sphere and column, then the volume of them could be reckoned conveniently. The mean volume of the PC particle in the extrudate (Fig. 4) is about 0.468 μm^3, while that of the fibril in Fig. 8c of GAIMP is about 2.791 μm^3 even if both ends of the fibrils beyond the micrograph are omitted. Besides, the mean volume of the fibril in Fig. 7 is also greatly larger than that of the PC sphere in Fig. 5 and Fig. 7. Obviously, the difference in the volume between the PC particle and the fibril reveals that a single fibril is not simply derived from a single PC particle during gas penetration. Interestingly, many ''strings of beads'' shown by the white arrows in Fig. 7d′ indicate that more PC particles had coalesced during gas penetration. The ''beads'' of the ''strings of beads'' are primarily of elliptical form, which might imply the following processes. First, the distance between the deformed PC particles decreased as PC spheres were elongated into ellipse. Then, these particles touched each other if the distance was short enough. As shown by the white arrows in Fig. 5b, 5b′, Fig. 7b, c, a few PC bars and fibrils are characterized with many protuberant humps on their bodies. It indicates that the fibrils came from the ''strings of beads'' once they were exposed to further shear field. However, the longer and slimmer fibrils in Fig. 7b′ have no visible humps, which may imply that shear rate is strong enough to turn the fibrils with humps in Fig. 7b into the longer and slimmer fibrils in Fig. 8b′. Thus, the process of the morphological development could be illustrated in Fig. 13. Based on it, the fibrillation of PC/PE blend in GAIM can be divided into three stages, (1) The PC particles turn into ellipses; (2) Ellipses impinge each other since the distance between them is decreased; (3). The coalesced particles

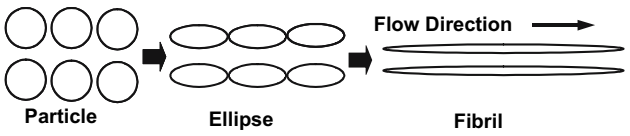

Fig. 13 Schematic diagram of morphological development of the PC particles in GAIM process

become fibrils due to further shear rate. As shown in Fig. 5a, 5a′, Fig. 7b, 7b′, the fibrils in the GAIMP are longer and more bulky than those in the SSP.

Previous studies might back up our viewpoint as well. [36, 37] It have been found that the amount of the fibrils is proportional to PC concentration, while the diameter of the fibrils becomes nonuniform with the increase of PC concentration. Particle-particle impingement (coalescence) has been demonstrated to play an important role in formation of the dispersed phase domains [35]. As the PC concentration increases, the probability of coalescence increases, which favourably leads to the formation of larger particles. In particular, when melt is in shear or elongational field, a significant potential occurs for particle-particles interactions and coalescence. And then it is possible for the coalesced particles to be deformed in shear or elongational field. Furthermore, although other studies [26, 35] didn't propose such two-step mechanism for PC particles deformation, they all regarded that PC phase is preferably deformed when its concentration is about 15–20%. And more or less than this value, PC fibrils are not easy to be fabricated.

Thus conclusion can be drawn: the PC spheres subjected to gas penetration are much easier to coalesce and fibrillate in GAIM than those in the SS process as well as in the CIM process. The gradient structure of GAIMP is somewhat different from that in our previous study [21], which is understandable in light of the complex processing parameters involved during GAIM process. We don't expect to get the absolutely same results in the similar study, but the explicit trend of morphology and the mechanism of the morphological formation in GAIM. In a word, in the present investigation, higher shear rate induced by gas penetration and the efficient cooling of the melt temperature are two critical factors to the gradient structure formation during the GAIM process. The former plays an essential role in the formation of PC fibrils, and the latter helps to preserve the fibrils formed.

Conclusions

Two kinds of specimens were prepared respectively by SS and GAIM process, namely SSP and GAIMP. Morphological observation reveals that they both assumed the ''skin-core'' structure because the PC phase, in different regions, all experienced different thermo-mechanical history during the above molding process. However, there are a few remarkable differences in the degree of deformation and the morphological distribution between SSP and GAIMP. For SSP, many short micro-fibers with the largest degree of deformation were just formed in sub skin, and the shape of the PC phase at the gate end changed more severely than that at the non-gate end. While for GAIMP, numerous slim fibrils with fairly large aspect ratio were formed in the core layer and sub-skin intermediate layer. Moreover, the fibrils in the core layer of the GAIMP, especially at the non-gate end, were much longer and more uniform than those in sub skin of SSP, which indicate that gas penetration is very efficient in assisting PC phase to fibrillate. Unexpectedly, the micro-fibers in the core layer of GAIMP, at the non-gate end, are much slimmer and more uniform than those in the corresponding layer at the gate end. Based on the analysis of the formation of the ''strings of beads'' in SSP and GAIMP, another conclusion could be obtained: PC particles exposed to gas penetration are much easier to coalesce and fibrillate during GAIM process.

Acknowledgements The authors gratefully acknowledge the financial support of the grand subject of the National Nature Science Foundation of China (Grant No. 10590351) and the Major State Basic Research Projects (Grant No. 2005CB623808). We also would like to thank Mr. Yu-Xin Liu, Zhen-Hong Liang, Hong-Hua Yang of Henan Xinxiang MEIDA plastics CO., LTD for their generous help in preparing specimens.

References

1. Rush KC (1989) Annual ANTEC-89 47th Annual Technical Conference of SPE, New York, 1014
2. Carl K (1991) Plast World 49:37
3. Michaeli W, Haberstroh E (2000) Kunststoffe Plast Europe 90:52
4. Chen SC, Hsu KS, Hung JS (1995) Ind Eng Chem Res 34:416
5. Chen SC, Hsu KF, Hsu KS (1995) J Appl Polym Sci 58:793
6. Turng LS, Wang VW (1991) SPE ANTEC Tech Pap 37:297
7. Chen SC, Cheng NT, Sheng HK (1996) Int J Mech Sci 38:335
8. Khayat RE, Derdouri A, Hebert LP (1995) J Non Newtonian Fluid Mech 22:253
9. Turng LS (1995) Process Eng Plast 8:171
10. Rothe J (1988) Kunstst Ger Plast 78:19
11. Li CT (2004) Polym Eng Sci 44:992
12. Zhou HM (2003) Polym Eng Sci 43:91
13. Chen SC, Cheng NT, Hsu KS (1995) Int Commun Heat Mass Transfer 22:319
14. Chen SC, Cheng NT (1996) Int Commun Heat Mass Transfer 23:215
15. Chen SC, Hung JS (1995) J App Polym Sci 58:793
16. Chien RD, Chen SC, Chen YC (2002) Plast Rubber Compos 31:336
17. Chen SC, Dong JG, Jong WR, et al (1996) SPE Tech Papers 43:663
18. Chien RD, Chen SC, Kang Y, et al (1998) J Reinf Plast Compos 17:1213

19. Grelle PF, Kallman MA, Talladge BJ (1994) Structural Plastics Conference and Parts Competition, Washington, 387
20. Hu SY, Chien RD, Chen SC, et al (1996) Plast Rub Compos Pro 26:172
21. Zheng GQ, Yang W, Yin B, Yang MB, et al (2006) J Appl Polym Sci 102:3069
22. Lee MP, Hiltner A, Baer E (1992) Polymer 33:675
23. Silverstenin MS, Hiltner A, Baer E (1991) J Appl Polym Sci 43:157
24. Claudia S, Achim RF, Gilner W, Goerg HM, et al (2005) Macromol Mater Eng 290:621
25. Tadmor Z (1974) J Appl Polym Sci 18:1753
26. Li ZM, Yang W, Yang SY, et al (2004) J Mater Sci 39:413
27. Fellahi S, Favis BD, Fisa B (1996) Polymer 37:2615
28. Pal SK, Kale DD (2000) J Polym Res 7:107
29. Lee MP, Hiltner A, Baer E (1992) Polymer 33:675
30. Liu SJ, Chen YS (2004) Compos Part A 35:177
31. Wang DY, Wang J, Qu XZ, et al (2000) Acta Polymerica Sinica 44:111
32. Delaby I, Ernst B, Froelich D, Muller R (1996) Polym Eng Sci 36:1627
33. Grace HP (1982) Chem Eng Commun 14:225
34. Gonzalez-Nunez R, De Kee D, Favis BD (1996) Polymer 37:4689
35. Xu HS, Li ZM, Pan JL, Yang MB, et al (2004) Macromol Mater Eng 289:1087
36. Chapleau N, Favis BD (1995) J Mater Sci 30:142
37. Favis BD (2000) In: Paul DR, Bucknall CD (eds) Polymer Blends, vol 1: Formulation. JohnWiley & Sons, New York, p 502